Effect of Some Compatibilizing Agents on Clay Dispersion of Polypropylene-Clay Nanocomposites

M. L. López-Quintanilla,[1] S. Sánchez-Valdés,[1] L. F. Ramos de Valle,[1] F. J. Medellín-Rodríguez[2]

[1]*Centro de Investigación en Química Aplicada (CIQA), P.O. Box 379, Saltillo, Coahuila 25100, México*
[2]*Centro de Investigación y Estudios de Posgrado/FCQ/UASLP, Av. Dr. Manuel Nava 6, Zona Universitaria, San Luis Potosi 78210, Mexico*

Received 1 July 2005; accepted 20 September 2005
DOI 10.1002/app.23262
Published online in Wiley InterScience (www.interscience.wiley.com).

ABSTRACT: Polypropylene (PP)-clay nanocomposites were obtained and studied by using three different coupling agents, glycidyl methacrylate (GMA), acrylic acid (AA), and maleic anhydride (MA). Three different clays, natural montmorillonite (Cloisite Na+) and chemically modified clays Cloisite 20A and Cloisite 30B, have also been used. Nanocomposites were prepared by melt-blending in a twin-screw extruder using two mixing methods: two-step mixing and one-step mixing. The relative influence of each factor was observed from structural analysis by WAXD, POM, TEM, and mechanical properties. The results were analyzed in terms of the effect of each compatibilizing agent and incorporation method in the clay dispersion and mechanical properties of the nanocomposite. Experimental results showed that clay dispersion and interfacial adhesion are greatly affected by the kind of matrix modification. The polarity and reactivity of polar groups give as a result better interfacial adhesion and subsequent mechanical performance. PP-*g*-GMA and PP-*g*-MA were better compatibilizing agents than PP-*g*-AA. Better dispersion and exfoliation for the nanoclays were obtained when using two-step mixing than one-step mixing conditions. J Appl Polym Sci 100: 4748–4756, 2006

Key words: nanocomposites; polypropylene; montmorillonite; glycidyl methacrylate; compatibilization

INTRODUCTION

Nanocomposites have received special attention because of their improved properties at very low loading levels compared with conventional filler composites. Among these improved properties are mechanical, dimensional, barrier to different gases, thermal stability, and flame retardant enhancements with respect to the bulk polymer.[1–4] The hydrophilic clay needs to be modified prior to its introduction in most organophilic polymer matrices, to achieve good interfacial adhesion and therefore a better mechanical performance. Clay modification is generally achieved by ion exchange reactions of organophilic cations for sodium ions.[5] Polymer-clay nanocomposites are usually divided into three general types: conventional composites, in which the clay acts as a normal filler; intercalated nanocomposites, in which a small amount of polymer moves into the gallery spacing between the clay pallets; and exfoliated nanocomposites, in which the clay pallets are fully dispersed in a continuous polymer matrix.[6–8] Several polymer nanocomposites have been reported, such as polyamides,[9] polystyrene,[10] polyurethane,[11] and thermosetting polymers such as phenol and epoxy resins.[12] Polypropylene (PP) exhibits an attractive combination of low cost, low weight, and extraordinary versatility in terms of properties, applications, and recycling.[13] However, because of the low polarity of this resin, it is difficult to get the exfoliated and homogenous dispersion of the clay layer at the nanometer level in the polymer matrix. This is mainly due to the fact that the silicate clay layers have polar hydroxyl groups and are compatible only with polymer containing polar functional groups. Consequently, the matrix modification with polar moieties is necessary prior to modified clay introduction to achieve nanometric dispersion of the clay.[14] With the enhancement of the clay dispersion, the aspect ratio of the particle is increased and the reinforcement effect is improved. When preparing nanocomposites by melt compounding, the exfoliation and dispersion of nanoclays in PP depend on the organic modifier of the nanoclay, the initial interlayer spacing, the concentration of functional groups in the compatibilizer and its overall concentration in the composite, the viscosity of the plastic resin, and the operational conditions, such as screw configurations of extruders, rpm, temperature, residence time, etc. Recently, the effects of extrusion compounding conditions upon the properties of nanocomposites have attracted significant inter-

Correspondence to: S. Sánchez-Valdés (saul@ciqa.mx).
Contract grant sponsor: CONACyT; contract grant number: SEP-2003-CO2–43983.

est.[15–18] The main conclusions of these studies are that sufficient long residence time is necessary to intercalate or exfoliate the nanoclays in the polymer matrix; excessive shear intensity could cause poor exfoliation; exfoliation of the clay in composites prepared in single-screw extruders is generally poorer than that in twin-screw extruders and that the clay could be exfoliated even at low shear rate when the process temperatures are high, due to the fact that the diffusion of polymers into the interlayers is enhanced. Even though shear is an important factor to achieve a good clay dispersion in the polymer, shear alone is not enough to provide nanometric dispersion of the clay. Interfacial adhesion needs to be higher to improve clay dispersion and therefore a better performance of the nanocomposite.

PP nanocomposites using modified clays have attracted much attention during the last few years, especially using maleic anhydride (MA) modified PP as a coupling agent.[19–24] PP-*g*-MA has been widely used in these systems because it offers an efficient level of intercalation/exfoliation, however MA groups are generally grafted at the end of the main PP chain that could limit its reactivity. Other coupling agents such as glycidyl methacrylate (GMA) and acrylic acid (AA) can homopolymerize and increase the number of functional groups attached to the polyolefin that could increase their capability to undergo specific interactions. In this work, three different polar coupling agents GMA grafted PP (PP-*g*-GMA), AA grafted PP (PP-*g*-AA), and MA grafted PP (PP-*g*-MA) have been used.

MA has been widely used as a compatibilizing agent for this kind of systems and is used as reference in this work. The PP-Clay nanocomposites have been obtained by melt compounding with three different commercial montmorillonite clays, in a twin-screw extruder using two mixing methods: one-step mixing and two-step mixing.

EXPERIMENTAL

Materials

Commercial homopolymer, PP HP423, used for this study was produced from Indelpro (Tamaulipas, Mexico) with an MFR of 3.2 g/10 min. Three different coupling agents were used: a commercial PP-*g*-MA with 1.0% of MA, Polybond 3200 from Crompton; a commercial PP-*g*-AA with 6.0% of AA, Polybond 1002 from Crompton; and a PP-*g*-GMA with 1.9% of GMA prepared by us. Three different commercial clays were used as received: an unexchanged natural montmorillonite (Cloisite Na+) and two modified with a quaternary ammonium salt (Cloisite 20A and Cloisite 30B) from Southern Clay Products Co. (Gonzalez, TX). The main characteristics of the materials used are listed in Table I. For the preparation of PP-*g*-GMA, GMA (97% purity) and styrene (99% purity) were purchased from Aldrich and used as received. The dycumyl peroxide (DCP) from Aldrich was used without further purification.

Preparation of PP-*g*-GMA

It is reported that the addition of styrene as a comonomer improves markedly the grafting yield of GMA and MA onto PP.[25–27] It is proposed that styrene reacts first with PP tertiary macroradicals and the resulting styryl radicals then copolymerize readily with GMA.[25] In other words, GMA is not grafted directly onto PP macroradical but via styrene and more specifically styryl macroradicals.

A Brabender-like apparatus was used to prepare PP-*g*-GMA with a chamber of 300 cm^3 with nitrogen flux and using two sigma rotors. Liquid monomers (6 phr of GMA and 6.15 phr of Styrene) and 0.4 phr of DCP were premixed with PP (202 g) at room temperature for about 20 min so as for them to be adsorbed by the polymer. The mixture was then charged to the mixing chamber, which was preheated to 180°C and mixing was continued for a period of 12 min at a roller speed of 60 rpm. This sample was purified to remove unreacted GMA and other secondary products such as homopolymerized GMA and/or styrene copolymerized with GMA. About 1.5 g of the product was dissolved in hot xylene (30 mL) by stirring for 1 h and precipitated with acetone (100 mL). The precipitate was filtered, washed several times with acetone, and dried under vacuum at 80°C overnight. A non-back-titration method was used to determine the amount of grafted GMA. A sample of the purified product (about 1 g) was dissolved in hot xylene (75 mL), then 5 mL of trichloracetic acid (TCA) (0.3*M* xylene solution) was added. The mixture was kept at 105°C for 120 min to achieve the complete reaction of TCA with grafted GMA. The solution was then precipitated in acetone with continuous stirring, filtered, and washed. The filtrate (TCA residue) was titrated with 0.1*M* KOH solution in methanol by using phenolphthalein as indicator. FTIR was also used to verify the grafting of GMA into PP. Purified samples were pressed into thin films at 195°C under 120 bars of pressure between two Teflon sheets. Figure 1 shows the IR spectrum of PP and GMA modified PP. It can be observed that in the PP sample there does not appear any significant stretching band between 1700 and 1800 cm^{-1} mean while in the PP-*g*-GMA sample, the peak at 1726.3 cm^{-1} corresponding to the stretching of the carbonyl group of GMA is quite noticeable. This band was used to verify and compare the amount of grafted GMA with the titration results.

TABLE I
Main Characteristics of the Materials Used

	Polymers			
	PP	PP-*g*-MA	PP-*g*-AA	PP-*g*-GMA
Grade	Valtec HP423	Polybond 3200	Poybond 1002	PP-*g*-GMA
Supplier	Indelpro	Crompton	Crompton	Prepared by us
MFR (190°C/2.16 kg) (g/10 min)	3.2[a]	110.1[a]	21.5[a]	5.8[a]
Mw (g/mol)	307 137[a]	95 804[a]	162 504[a]	190 409[a]
Density at 23°C (g/ml)	0.9	0.91	0.91	0.91[a]
Melting point (°C)	162[a]	157[a]	165[a]	159[a]
Grafting level (wt %)	N/A	1.0	6.0	1.9[a]

	Nanoclays		
	Nanoclay Can+	Nanoclay C20A	Nanoclay C30B
Supplier	Southern clay products	Southern clay products	Southern clay products
Organic modifier	Unexchanged natural MMT	Dimethyl, dehydrogenated tallow, quaternary ammonium chloride, where HT is hydrogenated tallow (65%C18, 30%C16, 5%C14); Anion: chloride	Methyl, tallow, bis-2-hydroxyethyl, quaternary ammonium chloride, where HT is hydrogenated tallow (65%C18, 30%C16, 5%C14); Anion: chloride
Structure of organic modifier	N/A	CH_3 | $CH_3—N^+—HT$ | HT	CH_2CH_2OH | $CH_3—N^+—HT$ | CH_2CH_2OH
X-ray d_{001} (Å)	11.7	24.2	18.5

[a]Data obtained in the lab.

Preparation of PP-clay nanocomposites

Nanocomposites were obtained by previous preparation of a master batch of compatibilizing PP and clay (60/40) by mixing in a Werner and Pfleiderer twin screw extruder with an $L/D = 29/1$ and $D = 30$ mm operating at 190–200°C and 50 rpm in corotating mode. The clay was added through a side feeder. Subsequently, the desired amount of pure PP, master batch, and grafted PP were mixed in the twin screw extruder at 190–210°C and 100 rpm for the one-step mixing. Then the samples were pelletized and mixed again passing through the twin-screw extruder in a two-step mixing at 190–210°C and 200 rpm. The composition of nanocomposites is detailed in Table II.

After being dried at 80°C for 16 h, pellets of the nanocomposites were injection-molded into test pieces for mechanical tests by using a Battenfeld injection molder. The temperature of the cylinder was 185–215°C and that of the mold was 40°C.

The exact amount of montmorillonite clay in each composite was measured by burning the samples in a thermogravimetry analysis TA Instruments TGA-Q500. The resulting value was corrected for loss of structural water that occurred during the incineration.

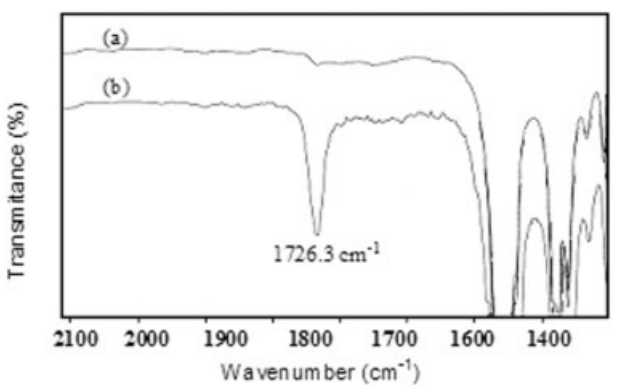

Figure 1 FTIR spectrum of (a) PP and (b) PP-*g*-GMA.

Evaluation of nanocomposites

X-ray diffraction of the clays and nanocomposites, to evaluate the evolution of the clay d_{001} reflection, was performed in a Siemens D5000 using Cu Kα X-ray radiation. The X-ray samples were obtained form compression molding to avoid the preferred orientation of the clay when samples are prepared from injection molding. Melt flow rate (MFR) was evaluated on the samples after one and two passes through the extruder according to ASTM D 1238. The mechanical

TABLE II
Sample Designation

Sample	PP (%)	PP-*g*- (wt %)	Type clay	Clay (wt %)	Clay by TGA (wt %)
PP	100	—	—	—	—
PP/PP-*g*-MA	84	PP-*g*-MA, 16	—	—	—
PP/PP-*g*-GMA	84	PP-*g*-GMA, 16	—	—	—
PP/PP-*g*-AA	84	PP-*g*-AA ,16	—	—	—
PP/PP-*g*-MA 4, Na+	84	PP-*g*-MA,12	Na+	4	3.10
PP/PP-*g*-MA 2, 20A	92	PP-*g*-MA, 6	20A	2	1.51
PP/PP-*g*-MA 4, 20A	84	PP-*g*-MA,12	20A	4	3.08
PP/PP-*g*-MA 6, 20A	76	PP-*g*-MA,18	20A	6	4.54
PP/PP-*g*-MA 4, 30B	84	PP-*g*-MA,12	30B	4	2.85
PP/PP-*g*-GMA 4, Na+	84	PP-*g*-GMA,12	Na+	4	3.18
PP/PP-*g*-GMA 2, 20A	92	PP-*g*-GMA, 6	20A	2	1.34
PP/PP-*g*-GMA 4, 20A	84	PP-*g*-GMA,12	20A	4	3.12
PP/PP-*g*-GMA 6, 20A	76	PP-*g*-GMA, 18	20A	6	4.60
PP/PP-*g*-GMA 4, 30B	84	PP-*g*-GMA,12	30B	4	2.78
PP/PP-*g*-AA 4, Na+	84	PP-*g*-AA,12	Na+	4	3.12
PP/PP-*g*-AA 2, 20A	92	PP-*g*-AA, 6	20A	2	1.50
PP/PP-*g*-AA 4, 20A	84	PP-*g*-AA,12	20A	4	2.98
PP/PP-*g*-AA 6, 20A	76	PP-*g*-AA, 18	20A	6	4.31
PP/PP-*g*-AA 4, 30B	84	PP-*g*-AA,12	30B	4	2.74

properties of the resulting nanocomposites, modulus, tensile strength, and elongation at break, were measured according to ASTM D 638 with an Instron Model 4301. Notched Izod Impact resistance was evaluated according ASTM D256. Ultrathin section for TEM analysis, ~70–100 nm in thickness, were cut from Izod bars, with a diamond knife using a Leica microtome. The TEM observations were performed for the thin sections of thin films with a Jeol-2000EX microscope with a field emission gun at a accelerating voltage of 200 kV.

RESULTS AND DISCUSSION

The actual clay content, as inorganic fraction, was found by TGA analysis in different parts of the samples and is listed in Table II. It can be seen in this table that the magnitude of variation of the clay content was around 25–30% less for the C20A samples and around 40% for the C30B samples. The final filler content determined by TGA, in all the samples, was less than the amount we added, perhaps because of the loss of filler during feeding and preparation of nanocomposites.

Table III shows the MFR results of the samples after one- and two-step mixing in the twin-screw extruder. It can be seen that after the second passing, the MFR increases in around 20% for all the PP-Clay nanocomposites indicating a lower viscosity related to the thermal degradation of the PP because of the increased residence time in the extruder. Mean while in the virgin PP and its blends with grafted PP, a more drastic increase in MFR is observed, around 40–50% of increase for the blends and around 60% of increase for the virgin PP, indicating a more drastic degradative chain scission process that reduces its molecular weight and viscosity. Although GPC data was not possible to obtain, the MFR results confirm the already accepted fact that the presence of nanoclay increases the viscosity of the blends. It can be observed that the percent change in MFR from step 1 to 2 is significantly reduced for the clay-containing samples and it could be related with the thermal stability of the clay as it was confirmed by other authors[28,29] who found that the incorporation of organo-montmorillonite into the PP matrix makes the TGA curves shift toward a high temperature zone. It also can be observed that the samples with C20A have in general lower MFR than that with C30B and CNa+ for both mixing steps, this could be indicating that C20A could be more exfoliated and more dispersed than C30B and CNa+. To verify the MFR results, TGA curves at a heating rate of

TABLE III
MFR Results (g/10 min)

Sample	1st step	2nd step	% Increase step1 to step2
PP	4.53	7.54	66
PP/PP-*g*-MA	6.57	9.95	51
PP/PP-*g*-GMA	4.05	5.70	41
PP/PP-*g*-AA	5.08	7.11	40
PP/PP-*g*-MA4, Na+	6.10	7.56	24
PP/PP-*g*-MA4, 20A	3.75	4.62	23
PP/PP-*g*-MA4, 30B	5.32	6.54	23
PP/PP-*g*-GMA4, Na+	4.00	5.02	25
PP/PP-*g*-GMA4, 20A	2.90	3.54	22
PP/PP-*g*-GMA4, 30B	3.85	4.81	25
PP/PP-*g*-AA4, 20A	4.82	5.78	20

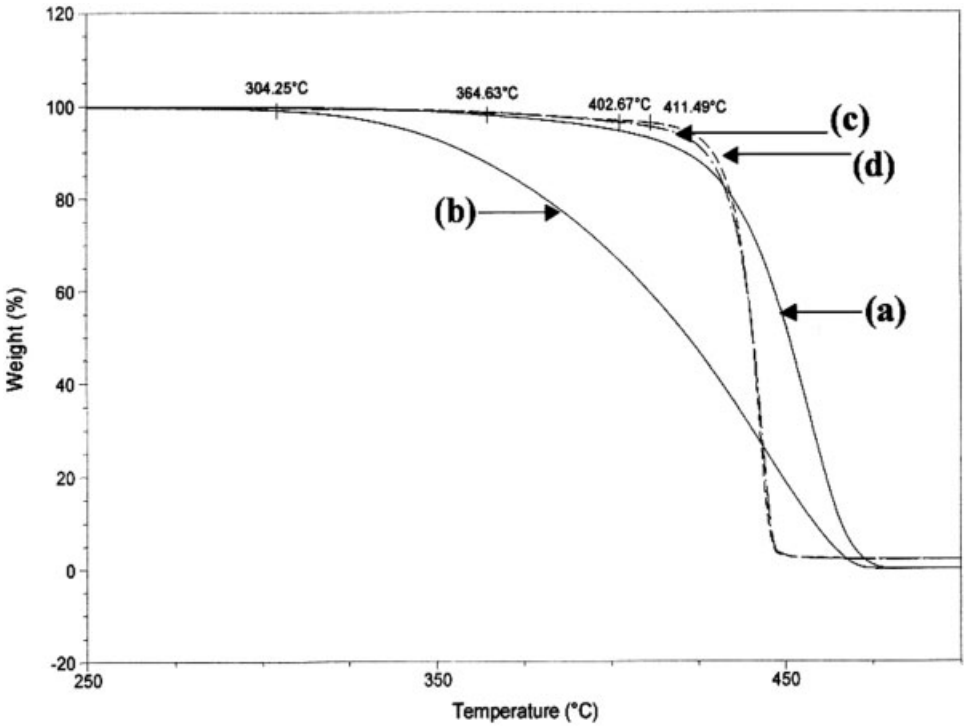

Figure 2 TGA curves of plain PP: (a) 1st step, (b) 2nd step and nanocomposites: (c) PP/PP-*g*-GMA, 4% 20A, 1st step, (d) PP/PP-*g*-GMA, 4% 20A, 2nd step.

10°C/min, as shown in Figure 2, were obtained from the thermal degradation of plain PP and nanocomposites containing 4% of C20A with PP-*g*-GMA as a coupling agent and two mixing conditions. The TG curve is a smooth weight-loss curve. It can be observed that the PP sample after the 2nd step mixing has lower degradation temperature than the 1st step mixing sample. The degradation temperature was reduced from 360°C for the 1st step to about 300°C for the 2nd step. It also can be observed that the incorporation of 20A clay into the PP matrix makes the TG curves shift toward the high-temperature zone. For the PP/Clay samples, the enhancement in thermal stability was about 45°C. It can be observed that the curves for 2nd step mixing samples are slightly shifted toward higher temperatures than the 1st step mixing samples. It is obvious from this figure that the incorporation of clay and its dispersion by mixing improves the thermal stability of PP. These results confirm the behavior observed in MFR where the percent of change in MFR from step 1 to 2 was significantly reduced for the clay-containing samples.

Table IV shows mechanical properties of the composites obtained for the 2nd step mixing, specifically Young's modulus, tensile strength, tensile strain, and notched Izod impact resistance. Analyzing the trends on mechanical properties gives information about the effect of compatibilizing agent, nanoclays, and processing method.

It can be seen, in Table IV, higher Young's modulus values when increasing the clay content from 2–6% being the most noticeable change at low clay contents (2%), with less drastic improvement with further addition of the clay content in all the coupling agents used. It can be seen that the higher values in Young's modulus are for the samples with PP-*g*-MA, and PP-*g*-GMA with C20A clay, an increase of around 35% of the value for simple PP, and the modulus is lower for the samples of PP-*g*-AA with this clay, only a 16% of increase compared with simple PP. It can also be found about the influence of the type of clay on mechanical performance, as all samples containing clay CNa+ and C30B have lower modulus than the samples containing C20A, in which higher modulus and tensile strength was observed.

The difference in mechanical performance shows the importance of the nature of the polyolefin grafting and the clay treatment process. Even though each of the compatibilizing polyolefin has different content of grafted polar groups, they were used at the same final composition in the nanocomposite. Both MA and GMA are more polar than AA. MA and GMA both have an instable ring that at elevated processing temperatures can easily be opened and undergo specific reactions, meanwhile AA has an open structure without a ring that limits its reactivity compared with MA and GMA groups. Because of this effect, GMA and MA shows a better compatibilizing effect, because the

TABLE IV
Mechanical Properties After 2nd Step Mixing

Sample	Modulus (MPa)	Tensile strength (Mpa)	Elongation at break (%)	Izod impact strength (J/m)
PP	1182 ± 28	32 ± 0.7	85	12.0 ± 0.3
PP/PP-*g*-MA	1190 ± 19	30 ± 1.0	90	13.2 ± 0.5
PP/PP-*g*-GMA	1188 ± 37	32 ± 0.5	85	12.5 ± 0.8
PP/PP-*g*-AA	1197 ± 31	31 ± 0.7	85	13.2 ± 0.3
PP/PP-*g*-MA4,Na+	1259 ± 42	32 ± 0.4	35	11.6 ± 0.2
PP/PP-*g*-MA2, 20A	1523 ± 15	35 ± 0.3	70	18.9 ± 0.3
PP/PP-*g*-MA4, 20A	1630 ± 21	38 ± 0.9	65	18.6 ± 0.5
PP/PP-*g*-MA6, 20A	1650 ± 35	39 ± 0.7	65	17.5 ± 0.8
PP/PP-*g*-MA4, 30B	1395 ± 32	34 ± 0.5	55	12.1 ± 0.3
PP/PP-*g*-GMA4, Na+	1308 ± 39	32 ± 0.9	45	12.9 ± 0.8
PP/PP-*g*-GMA 2, 20A	1519 ± 24	34 ± 0.5	70	18.5 ± 0.2
PP/PP-*g*-GMA 4, 20A	1602 ± 41	36 ± 0.6	60	17.7 ± 0.4
PP/PP-*g*-GMA 6, 20A	1629 ± 19	38 ± 0.7	55	16.8 ± 0.7
PP/PP-*g*-GMA4, 30B	1351 ± 22	33 ± 0.2	55	13.2 ± 0.5
PP/PP-*g*-AA 2, 20A	1289 ± 20	31 ± 0.4	55	15.3 ± 0.3
PP/PP-*g*-AA 4, 20A	1400 ± 25	33 ± 0.4	50	14.9 ± 0.7
PP/PP-*g*-AA 6, 20A	1425 ± 33	34 ± 0.7	50	13.5 ± 0.5

polar interactions with the polar clay are more favorable compared with PP-*g*-AA. Another feature that may explain the improved properties of PP-*g*-MA and PP-*g*-GMA compared with the other compatibilizing agents is the imide bond formation between nucleophile ammonium groups of the clay and MA groups and ring opening reaction for GMA. The modified clay surfactant, ammonium salt, exists in an acid-base equilibrium, being able to react as a nucleophile with the carbonyl groups on the grafting agent. The reactivity of MA and GMA carbonyl groups toward this kind of reactions is higher than in the case of AA at equal periods of time.

A more notorious increase in tensile strength was observed for the samples with MA and GMA with clay C20A, of around 12–16% of change compared with only 3% of increase of AA samples.

Elongation at break values show in general a decrease on elongation of the nanocomposite with most of the functionalized polymer used. This behavior is common in this kind of systems, since the clay could act as a defect affecting the deformation capability. However, the PP-*g*-MA and PP-*g*-GMA nanocomposites produce an increase on the modulus and stiffness and a less drastic reduction of the deformation properties. The addition of clay to PP improves the tensile modulus and tensile strength, but reduces the elongation at break, regardless of the coupling agent used.

Notched Izod impact strength values show in general an increase on the impact strength of the nanocomposites with all the compatibilizers used. It can be observed that the sample with MA and GMA are the ones with higher values on impact resistance. It can also be found about the influence of the kind of clay on impact resistance, as all samples with C20A have higher values of this property than the samples containing CNa+ and C30B.

The analysis of the mechanical properties of the nanocomposites show clearly the influence of the kind of compatibilizing agent in the final properties of the composite. GMA and MA has higher compatibilizing effect than AA because of their different polarity promoting a better mechanical performance specially in Young's modulus and Impact strength.

In the PP-*g*-GMA and Cloisite 20A nanocomposite X-ray diffraction patterns (Fig. 3), after one step of mixing, there can be observed an increase in intergallery spacing for all the clay contents, as the d_{001} peak shifts to lower angles. This increase is due to the PP and PP-*g*-GMA interaction between clay pallets. All the samples show a shift to lower angles and higher intergallery spacing of about 2.54° and 34.6 Å compared with 3.52° and 24.5 Å of the clay 20A.

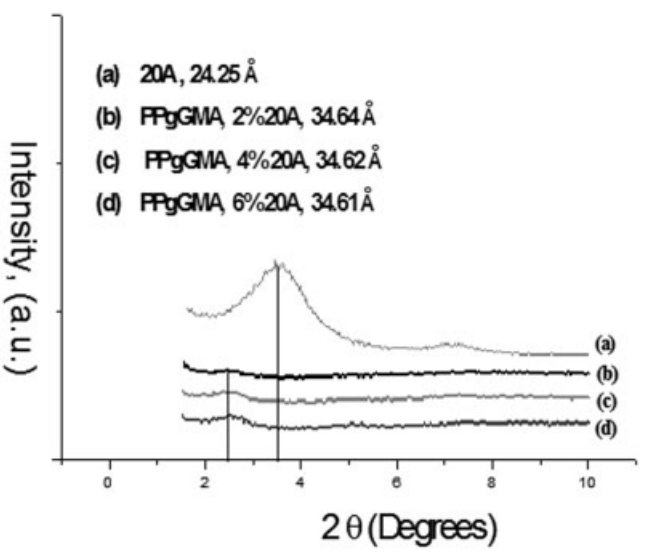

Figure 3 X-ray diffraction patterns of nanocomposites PP/PP-*g*-GMA and C20A with different content of clay.

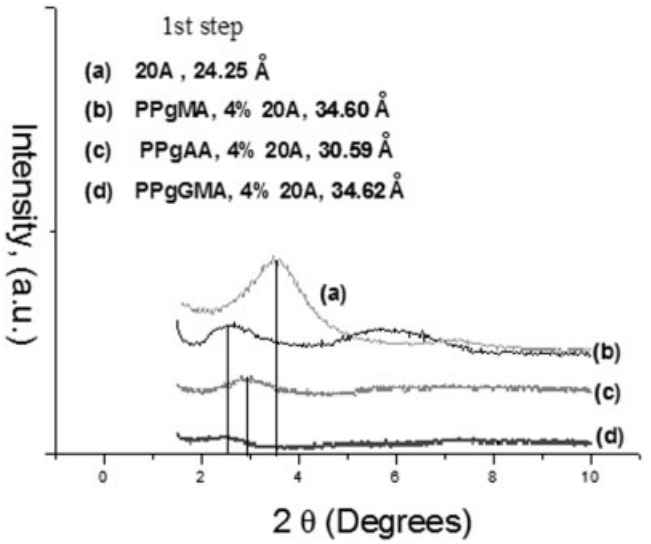

Figure 4 X-ray diffraction patterns of nanocomposites with different compatibilizing agent and 4% of C20A after 1st step mixing.

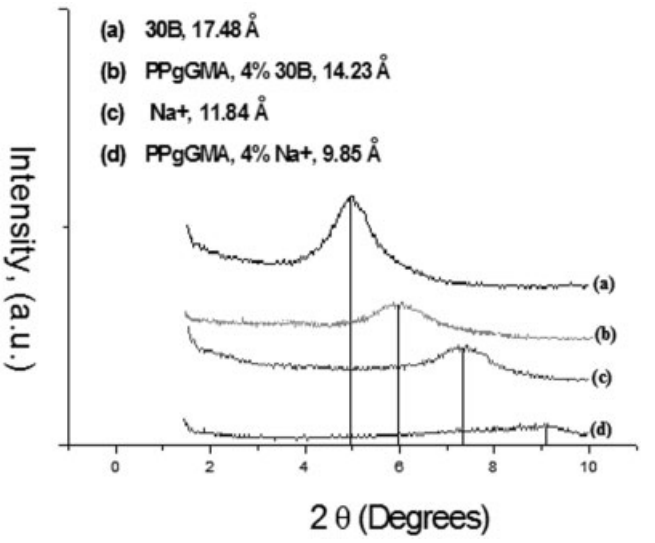

Figure 6 X-ray diffraction patterns of nanocomposites with different type of clay.

The X-ray diffraction patterns of nanocomposites with C20A and different grafted PP, obtained after one step of mixing, are shown in Figure 4. It can be observed that all the functionalized PP samples show the d_{001} peak at lower angles being more pronounced this shift with PP-*g*-GMA and PP-*g*-MA and the increase in intergallery spacing is more noticeable for samples containing GMA and MA than for the samples with AA.

The X-ray results for the 2nd step mixing (Fig. 5) show similar behavior than the 1st step but the shift of the d_{001} peak is more noticeable and the intergallery spacing is higher than that obtained for the 1st step mixing. This shift in the diffraction peak to lower 2θ value may not always offer evidence for exfoliation, but for ordered or disordered intercalation, which has been confirmed by various authors by TEM examination.

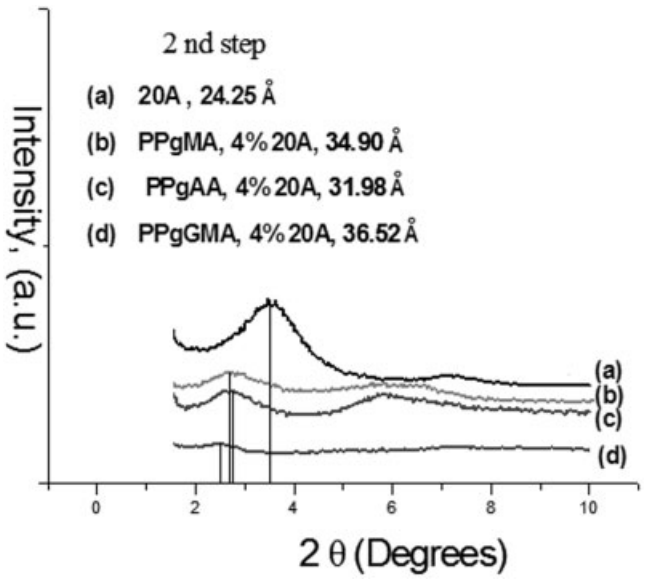

Figure 5 X-ray diffraction patterns of nanocomposites with different compatibilizing agent and 4% of C20A after 2nd step mixing.

The X-ray results for the nanocomposites with PP-*g*-GMA and different type of clay obtained after one step of mixing are shown in Figure 6. It was expected that C30B would have better exfoliation and dispersion in PP because the organic modifier of this clay has two ethoxy groups (Table I), which should have stronger interactions with the grafting PP. However, the samples with clay 30B show a d_{001} peak shift to higher angles with an intergallery spacing smaller than the original clay, indicating a poor exfoliation of this clay and less effective reinforcement in mechanical properties as was observed in Table IV. This is consistent with the studies of Lee et al.[30] who found that in composites of PP/PP-*g*-MA/C30B prepared at 210°C in a Brabender mixer at 50 rpm, the X-ray diffraction patterns showed that the intergallery spacing was smaller than the original spacing of the clay. The authors explained that the partial exfoliation of this clay (C30B) in PP was due to its poor thermal stability and its initial smaller interlayer spacing. The effect of residence time, temperatures, and shear rate in the presence of oxygen may result in lower thermal stabilities when using the extrusion conditions that we used in this work, which is in agreement with the observations of these authors. Meanwhile, for the samples with Na+, the shift is to higher angles and the spacing appears at lower values. This confirms that no exfoliation could be achieved by using the CNa+ clay and

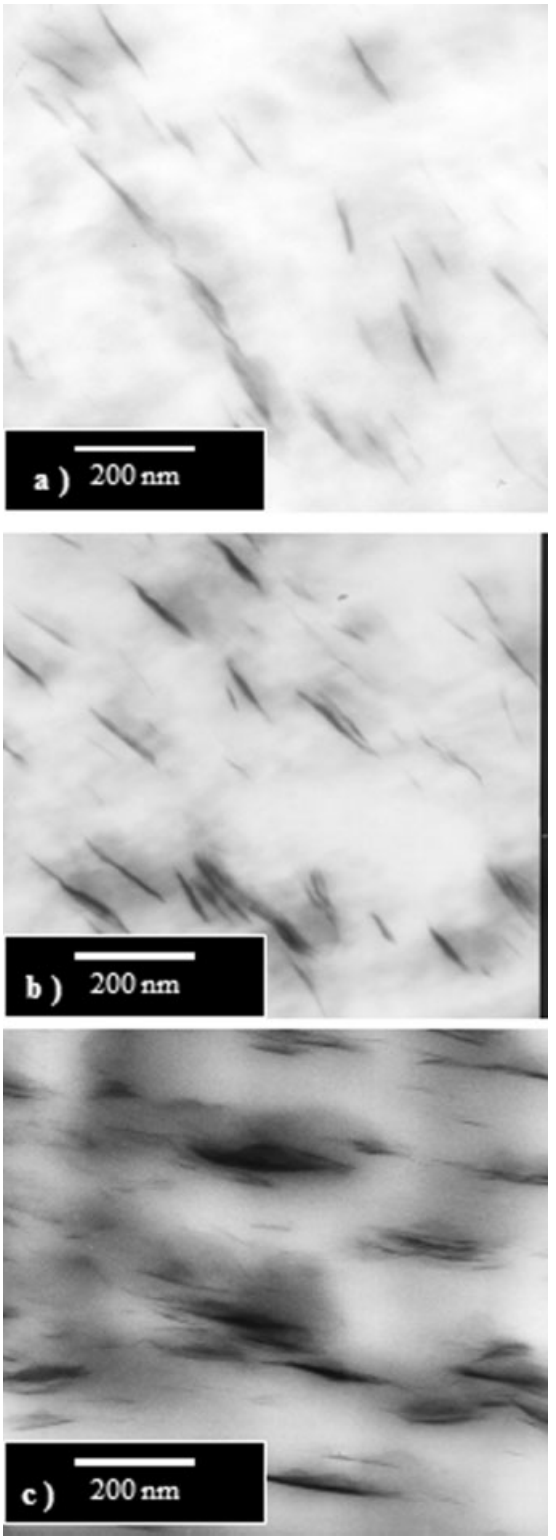

Figure 7 TEM images of nanocomposites with C20A at 4% and (a) PP/PP-*g*-MA, (b) PP/PP-*g*-GMA, and (c) PP/PP-*g*-AA.

that this clay is less effective in the reinforcement of the nanocomposites as was observed in mechanical properties. This is in agreement with the results from other authors[31] and could be related with the dehydration during heating as was reported by Brindley and Brown.[32] Since no exfoliation could be achieved by using the C30B and CNa+ clays, composites of these materials were not evaluated further.

TEM micrographs of nanocomposites based on C20A clay and the different grafted polypropylenes, shown in Figure 7, provide a direct visualization of the degree of organoclay exfoliation in these materials. These images are in good agreement with observed mechanical properties. The clay layers were exfoliated and dispersed to the monolayer in the MA and GMA samples. MA (a) and GMA nanocomposites (b) show similar morphology with a higher degree of disordered structures and exfoliated layers than AA nanocomposites (c). It can be observed that a slightly more exfoliated samples were obtained when using PP-*g*-MA than PP-*g*-GMA. These photographs showed that the thickly stacked layer structures were separated into thinner ones when using PP-*g*-MA and PP-*g*-GMA through the processing of the nanocomposite, though not so perfectly dispersed PP-*g*-AA samples in which still stacks or tactoids of the clay are observed. This result shows the intercalation effect of the polar groups in MA and GMA compared with AA.

CONCLUSIONS

In this study, GMA, AA, and MA modified PP nanocomposites have been obtained and three different clays have been used. PP-*g*-GMA and PP-*g*-MA were better compatibilizing agents than PP-*g*-AA. The incorporation of clay fillers into the PP matrix enhances the thermal stability of PP. Clay dispersion and interfacial adhesion are greatly affected by the kind of matrix modification. Both, clay modification and processing conditions are important in achieving an appropriated nanometric dispersion of clay layers and a homogeneous distribution of the clay in the sample. The polarity and reactivity of polar groups give as a result better interfacial adhesion and subsequent mechanical performance. The two-step mixing conditions results in better dispersion and exfoliation for the nanofillers than one-step mixing.

The authors want to acknowledge the support of Ing. Adriana Espinoza and Flora Beltran, and the technical support of Blanca Huerta, Josefina Zamora, Concepcion Martinez, Rodrigo Cedillo, Sandra Peregrina, Jesus Rodriguez, and Aracelly Patrón.

References

1. Garcia, L. D.; Picazo, O.; Merino, J. C.; Pastor, J. M. Eur Polym J 2003, 39, 945.
2. Zanetti, M.; Lomakin, S.; Camino, G. Macromol Mater Eng 2000, 279, 1.
3. Kato, M.; Usuki, A.; Okada, A. J Appl Polym Sci 1997, 66, 1781.

4. Alexandre, M.; Dubois, P. Mater Sci Eng R Rep 2000, 26, 1.
5. Krishnamoorti, R.; Vaia, R. A.; Giannelis, E. P. Chem Mater 1996, 9, 1728.
6. Lan, T.; Pinnavaia, T. Chem Mater 1994, 6, 2216.
7. Jeon, H. G.; Jung, H. T.; Lee, S. D. Polym Bull 1998, 41, 107.
8. Zhu, L.; Xanthos, M. J Appl Polym Sci 2004, 93, 1891.
9. Uzuki, A.; Kawasumi, M.; Kojima, Y.; Fukushima, Y.; Okada, A.; Karauchi, T.; Kamigaito, O. J Mater Res 1993, 8, 1179.
10. Vaia, R.; Isii, H.; Giannelis, E. Chem Mater 1993, 5, 1694.
11. Yano, K.; Usuki, A.; Okada, A.; Kurauchi, T.; Kamigatio, O. J Polym Sci Part A: Polym Chem 1993, 31, 2493.
12. Wang, M.; Pinnavaia, T. J Chem Mater 1994, 6, 468.
13. Moore, E. Polypropylene Handbook; Hanser: Munich, 1996.
14. Manias, E.; Touny, A.; Wu, L.; Lu, B.; Strawhecker, K.; Guilman, J.; Chung, T. Polym Mater Sci Eng 2000, 82, 282.
15. Andersen, P. Soc Plast Eng Annu Tech Conf 2002, 219.
16. Cho, J. W.; Logsdon, J.; Omachiniski, S.; Qian, G.; Lan, T.; Wormer, T. W.; Smith, W. S. Soc Plast Eng Annu Tech Conf 2002, 214.
17. Dennis, H. R.; Hunter, D. L.; Chang, D.; Kim, S.; White, J. L.; Cho, J. W.; Paul, D. R. Polymer 2001, 42, 9513.
18. Kwak, M.; Lee, M.; Lee, B. Soc Plast Eng Annu Tech Conf 2002, 224.
19. Svoboda, P.; Zeng, Ch.; Wang, H.; Lee, L. J.; Tomasko, D. L. J Appl Polym Sci 2002, 85, 1562.
20. Kim, Y; White, J. L. J Appl Polym Sci 2005, 96, 1888.
21. Ton-That, M. T.; Perrin-Sarazin, F.; Cole, K. C.; Bureau, M. N.; Denault, J. Polym Eng Sci 2004, 44, 1212.
22. Utraki, L. A.; Simha, R. Macromolecules 2004, 37, 10123.
23. Chen, L.; Wong, S. Ch.; Pisharath, S. K. J Appl Polym Sci 2003, 88, 3298.
24. Vaxman, A.; Tsalic, N.; Benderly, D.; Shalom, R.; Narkis, M. Soc Plast Eng Annu Tech Conf 2004, 1887.
25. Cartier, H.; Hu, G. H. J Polym Sci Part A: Polym Chem 1998, 36, 1053.
26. Cartier, H.; Hu, G. H. J Polym Sci Part A: Polym Chem 1998, 36, 2763.
27. Sun, Y. J; Hu, G. H.; Lambla, M. J Appl Polym Sci 1995, 57, 1043.
28. He, J. D.; Cheung, M. K.; Yang, M. S.; Qi, Z. J Appl Polym Sci 2003, 89, 3404.
29. Zanetti, M.; Camino, G.; Toman, R.; Mulhaupt, R. Polymer 2001, 42, 4501.
30. Lee, J.; Lim, Y.; Park, O. Polym Bull 2000, 45, 191.
31. Gopakumar, T. G.; Lee, J. A.; Kontopoulou, M.; Parent, J. S. Polymer 2002, 43, 5483.
32. Brindley, G.W.; Brown, G. Crystal Structures of Clay Minerals and Their X-Ray Identification; Mineralogical Society: London, 1980.